

See discussions, stats, and author profiles for this publication at: <https://www.researchgate.net/publication/231238288>

# Chemical Synthesis of a Polyaniline/Gold Composite Using Tetrachloroaurate

ARTICLE *in* CHEMISTRY OF MATERIALS · JULY 2004

Impact Factor: 8.35 · DOI: 10.1021/cm049478i

---

CITATIONS

123

---

READS

20

## 2 AUTHORS:



**John Kinyanjui**

Professional Consulting

**18** PUBLICATIONS **372** CITATIONS

SEE PROFILE



**David W Hatchett**

University of Nevada, Las Vegas

**41** PUBLICATIONS **1,459** CITATIONS

SEE PROFILE

# Chemical Synthesis of a Polyaniline/Gold Composite Using Tetrachloroaurate

John M. Kinyanjui and David W. Hatchett\*

Department of Chemistry, University of Nevada, Las Vegas, 4505 Maryland Parkway,  
Las Vegas, Nevada 89154-4003

J. Anthony Smith and Mira Josowicz

Department of Chemistry and Biochemistry, Georgia Institute of Technology,  
Atlanta, Georgia 30332-0400

Received March 26, 2004. Revised Manuscript Received June 21, 2004

The chemical synthesis of polyaniline (PANI) is explored using tetrachloroaurate,  $\text{AuCl}_4^-$ . These studies provide a simple method for the oxidation of aniline by  $\text{AuCl}_4^-$  and simultaneous formation of bulk quantities of a PANI/Au composite. In situ UV/vis spectroscopy indicates that the rate of formation of gold colloids and intermediate (short-chain) PANI species is rapid in comparison to that of the long-chain PANI. Longer PANI chains are produced at a slower rate, at the expense of short-chain intermediate species. The gold particles act as nucleation sites for the oxidative formation of PANI, encapsulating the metal in the form of a polymer/metal composite. Results from the elemental analysis and the FTIR spectra of the composite material are consistent with PANI produced using only ammonium persulfate as the oxidant. In addition, XPS, optical microscopy, and TEM diffraction show that the gold particles are polycrystalline with relatively constant diameter (0.8–1  $\mu\text{m}$ ). Finally, the PANI/Au/ $\text{HBF}_4$  conductance does not change significantly with the introduction of Au particles, relative to that of PANI/ $\text{HBF}_4$  without Au particles. These studies provide a new method for growth of PANI/metal composites where the presence of the metal in the polymer does not adversely affect the electronic structure.

## Introduction

The synthesis and characterization of polyaniline (PANI) using a variety of synthetic methods and analysis techniques is well documented.<sup>1–4</sup> More recently PANI/metal composite properties have been investigated. For example, the electrocatalytic properties and sensing applications of PANI/ $\text{Pt}^{5-13}$  and PANI/ $\text{Pd}^{14-18}$

have been examined. In many cases the incorporation of metal clusters in the polymer matrix also provides discrete reaction sites that can be probed electrochemically.<sup>5–16</sup> However, the use of metal clusters in polymer matrixes to explore metal–ligand interactions in solution has been largely overlooked in the literature. The PANI/Au system is of particular interest because of the ability to spontaneously form thiol monolayers on gold surfaces. For example, ferrocene-tagged thiol monolayers have been used as chemical transducers for flow injection analysis of redox molecules.<sup>19</sup> We are particularly interested in using PANI/Au/thiol with designed functionality and tailored chemistry at the gold interface. These studies are beyond the scope of this paper and will be the focus of further studies. However, to accomplish such studies it is important to produce the PANI/Au without dramatically changing the doping or oxidation state of the polymer, which are critical in maintaining the high conductance of the material.

- (1) Huang, W.-S.; Humphrey, B. D.; MacDiarmid, A. G. J. *Faraday Discuss. Chem. Soc.* **1986**, *82*, 2385.
- (2) Heeger, A. J. *Synth. Met.* **1993**, *55–57*, 3471.
- (3) MacDiarmid, A. G. *Synth. Met.* **1997**, *84*, 27.
- (4) MacDiarmid, A. G.; Epstein, A. J. *Synth. Met.* **1995**, *69*, 85.
- (5) Kost, K. M.; Bartak, D. E.; Kazee, B.; Kuwana, T. *Anal. Chem.* **1988**, *60*, 2379.
- (6) Kitani, A.; Akashi, T.; Sugimoto, K.; Ito, S. *Synth. Met.* **2001**, *121*, 1301.
- (7) Coutanceau, C.; Croissant, M. J.; Napporn, T.; Lamy, C. *Electrochim. Acta* **2001**, *46*, 579.
- (8) Lai, E. K. W.; Beattie, P. D.; Holdcroft, S. *Synth. Met.* **1997**, *84*, 87.
- (9) Kao, W.-H.; Kuwana, T. *J. Am. Chem. Soc.* **1984**, *106*, 473.
- (10) Ficicioglu, F.; Kadigan, F. J. *Electroanal. Chem.* **1997**, *430*, 179.
- (11) Wang, Y.; Huang, J.; Zhang, C.; Wei, J.; Zhou, X. *Electroanalysis* **1998**, *10*, 776.
- (12) Conn, C.; Sestak, S.; Baker, A. T.; Unsworth, J. *Electroanalysis* **1998**, *10*, 1137.
- (13) Zhang, Z.-R.; Bao, W.-F.; Liu, C.-C. *Talanta* **1994**, *41*, 875.
- (14) Maksimov, Y. M.; Kolyadko, E. A.; Shishlova, A. V.; Podlovchnko, B. I. *Russ. J. Electrochem.* **2001**, *37*, 777.
- (15) Hasik, M.; Drelinkiewicz, A.; Choczynski, M.; Quillard, S.; Pron, A. *Synth. Met.* **1997**, *84*, 93.

- (16) Drelinkiewicz, A.; Hasik, M.; Kloc, M. *Catal. Lett.* **2000**, *64*, 41.
- (17) Josowicz, M.; Li, H.-S.; Domansky, K.; Baer, D. R. *Electroanalysis* **1999**, *11*, 10.
- (18) Kang, E. T.; Ting, Y. P.; Neoh, K. G.; Tan, K. L. *Synth. Met.* **1995**, *69*, 477.
- (19) Radford, P. T.; Creager, S. E. *Anal. Chim. Acta* **2001**, *449* (1–2), 199.

Previous studies examining the interaction between tetrachloroaurate ( $\text{AuCl}_4^-$ ) and conductive polymers such as polyaniline<sup>18,20,21</sup> and polypyrrole<sup>18</sup> have focused on the sorption properties of the materials. The processes rely on the preformed polymer's ability to reduce  $\text{AuCl}_4^-$ .<sup>18,20,21</sup> Accumulation of gold in the sorption process has been reported to be as high as 5 times the original polymer weight.<sup>19</sup> However, lack of chemical control of the gold/polymer sorption process at the imino nitrogen remains a key limitation of such processes. If the goal is to produce uniform metallic clusters encapsulated in the polymer matrix, then sorption processes are not adequate. Specifically, the dispersion of the metal in the polymer is limited because the  $\text{AuCl}_4^-$  typically reduces at the point of contact rather than dispersing into the polymer matrix.<sup>22</sup> If the goal is a homogeneous mixture of intrinsically conducting polymer with evenly dispersed gold clusters, more novel techniques must be employed in the synthesis of the composite.

Electrochemical methods offer precise control of the polymer oxidation state, thus influencing the degree of interaction between the polymer and the metal chloride anions such as  $\text{AuCl}_4^-$ . Composites of PANI with Pt,<sup>5</sup> Au,<sup>23</sup> Ag,<sup>24</sup> and Pd<sup>25</sup> have been produced using electrochemical methods. Diffusion of the metallic ions into the membrane occurs as the oxidation of the polymer progresses to restore charge neutrality in the system. Potential-dependent uptake and reduction of  $\text{AuCl}_4^-$  ions has been utilized to form gold clusters with variable dimensions within the polymer matrix.<sup>23</sup> The  $\text{AuCl}_4^-$  ions are reduced at potentials that are approximately 70 mV lower than the uptake potential for the anion. The potential-dependent formation of a PANI/Au composite has limitations. The quantity of composite produced is limited by the electrode's geometric area. In addition, the polymer/metal interface must withstand processing if the material is to be used on external devices. Finally, the composite formed in the electrochemical reaction contains more oxidized units in comparison to the polymer prior to the reduction of  $\text{AuCl}_4^-$ .<sup>23</sup> The oxidation state of the polymer is one parameter which has been shown to directly influence the conductance of PANI.<sup>49</sup>

Although the chemical synthesis of polyaniline using oxidizing agents such as ammonium peroxydisulfate<sup>26–28</sup> is well characterized, the synthesis and mechanism of polyaniline using  $\text{AuCl}_4^-$  are inherently more complex. For example, issues such as the final oxidation state of the metal and polymer, degree of proton doping, degree

of incorporation of the metal into the polymer matrix, and chemical composition of the polymer must be addressed. In this paper we describe a new synthetic route for the direct synthesis of a PANI/Au composite using  $\text{AuCl}_4^-$  as the oxidizing agent in solutions containing the acid  $\text{HBF}_4$ . The synthetic process is detailed, and the chemical characteristics of the system are evaluated and compared to those of PANI doped with only  $\text{HBF}_4$ . The in situ UV/vis studies are used to monitor the rate of formation of the products, and a synthetic mechanism is proposed on the basis of these results. In addition, optical imaging and TEM diffraction are used to probe the metal distribution, size, and crystallinity of Au in the PANI matrix. FTIR and XPS studies are used to examine the chemical properties of the polymer with and without Au clusters. Finally the sheet conductances of PANI/ $\text{HBF}_4$  and PANI/Au are investigated using a four-point resistance/conductance probe.

## Experimental Section

**Chemicals and Solutions.** Tetrafluoroboric acid,  $\text{HBF}_4$  (Aldrich, 44 wt %, catalog no. 20,793-4), potassium tetrachloroaurate,  $\text{KAuCl}_4$  (Aldrich, 98%, catalog no. 33,454-5), ammonium peroxydisulfate,  $(\text{NH}_4)_2\text{S}_2\text{O}_8$  (Mallinckrodt, catalog no. 7277-54-0), and aniline,  $\text{C}_6\text{H}_5\text{NH}_2$  (Aldrich, 99.9%, catalog no. 13,293-4) were used as received. All solutions were prepared using  $18.3 \text{ M}\Omega\cdot\text{cm}$  water obtained from a Barnstead E-pure water filtration system.

**PANI/Au Composite Material Synthesis.** A bulk PANI/Au composite used for FTIR and XPS measurements was produced by mixing 20 mL of  $\text{KAuCl}_4$  ( $2.5 \times 10^{-2} \text{ M}$ ) with 20 mL of 0.25 M aniline both dissolved in 1 M  $\text{HBF}_4$ , representing a mole ratio of  $\sim 1:10$  ( $\text{KAuCl}_4$  to aniline). The material was allowed to settle for 24 h and then collected using vacuum filtration, washed copiously with water, and dried under ambient conditions. Optical inspection shows no salt crystals formed on the surface from residual electrolyte. The filter paper had pore diameters on the order of  $3 \mu\text{m}$ . For comparison, the gold particle size was on the order of  $0.8\text{--}1 \mu\text{m}$  (verified by SEM and optical microscopy). Therefore, any free gold not encapsulated by the polymer could be washed through the filter paper during the rinsing cycles. Samples were also dried in a vacuum oven at  $\sim 70^\circ\text{C}$  prior to performance of the FTIR, XPS, and elemental analysis experiments. The synthetic process was repeated and resulted in an average product mass of  $0.0780 \text{ g} \pm 1.25\%$ . The weight of the product showed no acid concentration dependence.  $\text{HBF}_4$  was chosen because it does not degrade the polymer in the same manner observed for acids such as  $\text{H}_2\text{SO}_4$  and  $\text{HCl}$ .<sup>27</sup> Pure PANI samples without gold were synthesized via previously published methods using 0.25 M ammonium peroxydisulfate as an oxidant in 1 M  $\text{HBF}_4$ .<sup>27</sup>

**Elemental Analysis.** The analysis was conducted for C, N, H, Cl, F, and S by Atlantic Micro Labs, P.O. Box 2288, Norcross, GA 30091. A 50 mg sample was analyzed per run. Estimates for B were obtained using the known stoichiometry of  $\text{BF}_4^-$  and the elemental analysis data for fluorine.

**UV/Vis Spectroscopy.** All spectra were obtained using a StellarNet EPP2000 fiber optic spectrophotometer equipped with a D<sub>2</sub> lamp and tungsten filament source that were coupled into a single fiber. The transmitted light was collected after it passed through the cuvette by a second fiber and relayed to the detector. The integration time for the detector was typically 200 ms. The data acquisition times were varied to minimize the volume of data collected and stored. All UV/vis measurements were performed in a single, Teflon-capped, quartz cuvette with a 1 cm path length. The in situ characterization of reactants and products was performed using an episodic data capture routine. The data were collected at regular

(20) Kang, E. T.; Ting, Y. P.; Neoh, K. G.; Tan, K. L. *Polymer* **1993**, *34*, 4994.

(21) Ting, Y. P.; Neoh, K. G.; Kang, E. T.; Tan, K. L. *J. Chem. Technol. Biotechnol.* **1994**, *59*, 31.

(22) Smith, J. A.; Josowicz, M.; Janata, J. *J. Electrochem. Soc.* **2003**, *150*, E384.

(23) Hatchett, D. W.; Josowicz, M.; Janata, J. *Chem. Mater.* **1999**, *11*, 2989.

(24) Tian, Z. Q.; Lian, Y. Z.; Wang, J. Q.; Wang, S. J.; Li, W. H. *J. Electroanal. Chem.* **1991**, *308*, 357.

(25) Li, H.-S.; Josowicz, M.; Baer, D. R.; Engelhard, M. H.; Janata, J. *J. Electrochem. Soc.* **1995**, *142*, 798.

(26) Angelopoulos, M.; Asturias, G. E.; Ermer, S. P.; Ray, A.; Scherr, E. M.; Macdiarmid, A. G.; Akhtar, M.; Kiss, Z.; Epstein, A. J. *Mol. Cryst. Liq. Cryst.* **1988**, *160*, 151.

(27) Quillard, S.; Louarn, G.; Lefrant, S.; Macdiarmid, A. G. *Phys. Rev. B* **1994**, *50*, 12496.

(28) Syed, A. A.; Dinesan, M. K. *Talanta* **1991**, *38*, 815.

intervals using an integration time of 28 ms per scan. The episode capture time was initially 0.5 s to ensure that changes in solution conditions were monitored with sufficient spectroscopic detail.

The in situ UV/vis samples were prepared and monitored using 0.20 mL of  $2.50 \times 10^{-2}$  M  $\text{KAuCl}_4$  and 3.00 mL of 0.02 M aniline in 0.10 M  $\text{HBF}_4$ . A large excess of aniline was used to facilitate the complete reaction of the  $\text{KAuCl}_4$ . However, the overall concentration of each species in the cuvette was lowered to ensure optical transparency and the ability to obtain a measurable signal throughout the reaction. The solution conditions employed were used to keep the magnitude of the signal below 2 absorbance units at all times.

**FTIR Spectroscopy.** All FTIR measurements were performed using a BIO-RAD FTS-7000 spectrometer using a photoacoustic detector. Each sample was scanned 64 times with a resolution setting of  $4 \text{ cm}^{-1}$  and averaged to produce each spectrum. All samples were vacuum-dried overnight prior to measurement.

**Optical Imaging.** Optical images of the composites were obtained using an Olympus BX41 optical microscope. The optical dimensions of the microscope image were determined using a 0.1 mm per division standard. For example, the  $100\times$  objective provides a viewing area of  $9625 \mu\text{m}^2$  based on the  $x$  and  $y$  axis dimensions ( $x = 110 \mu\text{m}$ ,  $y = 87.5 \mu\text{m}$ ). The images were obtained using an Olympus DP-11 2.5 megapixel color CCD digital camera in the transmission light mode.

**Transmission Electron Microscopy.** TEM samples were placed on a copper grid in a dry state and then mounted in a holder. The images were made in the selected area in normal diffraction mode using a selected area diffraction aperture on a Hitachi HF2000 field emission gun transmission electron microscope poised at 200 kV.

**X-ray Photoelectron Spectroscopy.** XPS data were collected using a Surface Science SSX-100 system with an Al  $K\alpha$  X-ray excitation source (1486.67 eV). The system was equipped with a hemispherical electron analyzer with a position-sensitive anode. The polyaniline/gold powder samples were mounted on a double-sided carbon tape placed on a piece of aluminum foil. A background of the carbon tape was subtracted from the XPS results. For this study the carbon 1s peaks were assigned a binding energy of 284.6 eV and used as the energy reference. A chamber pressure of  $5 \times 10^{-9}$  Torr or lower was maintained for each sample measurement. The oxygen content for each sample was obtained from integration of the oxygen peak in XPS data and referenced versus nitrogen to provide an estimate for use in elemental analysis calculations.

**Conductance Measurements.** A 1.25 cm radius pellet was pressed from each material using 3 metric tons of pressure. The contacts were made using a Cascade Microtech C4S-64/50 probe head with tungsten carbide electrodes. The four-point probe sheet resistance of each pellet was then measured at locations across the surface of the pellet using an HP 34401A digital multimeter connected through a Cascade Microtech CPS-05 probe station. Constant pressure for each measurement was maintained for the probed head contacting the substrate. A total of at least five measurements at different locations are presented with representative standard deviations and relative standard deviations.

## Results and Discussion

**PANI/Au Synthesis.** The spectra of the reactants, reaction products, and reaction filtrate are presented in Figure 1. The reactants aniline and  $\text{AuCl}_4^-$  are presented in parts a and b, respectively, of Figure 1. Both reactants have UV/vis absorbance bands between 200 and 290 nm, which makes distinguishing the changes in the concentration of these species difficult. The aniline and  $\text{AuCl}_4^-$  bands are centered at 260 and 311.7 nm, respectively. The absorbance band for  $\text{AuCl}_4^-$  can be examined prior to and after completion of the

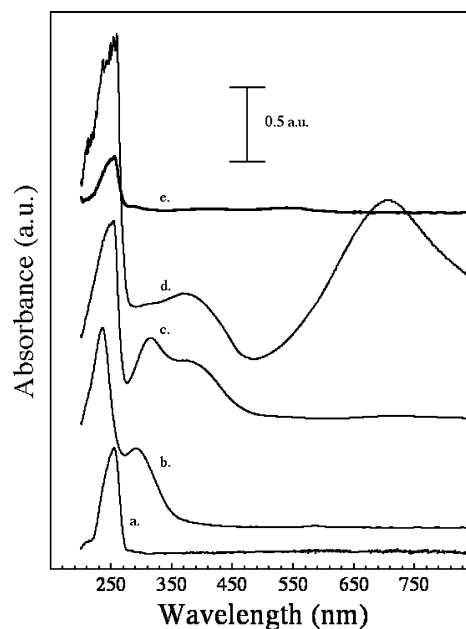


**Figure 1.** Bottom to top, UV/vis spectra of (a) 0.02 M aniline in 0.10 M  $\text{HBF}_4$ , (b) 2 mM  $\text{KAuCl}_4$  in 0.1 M  $\text{HBF}_4$ , (c) chemically synthesized PANI/Au colloid in aqueous solution obtained by mixing 0.2 mL of  $2.5 \times 10^{-2}$  M  $\text{KAuCl}_4$  and 3 mL of 0.02 M aniline in 0.1 M  $\text{HBF}_4$  at time 10 s, (d) same conditions as (c), data acquired at time 70 s, and (e) the solution after PANI precipitation and filtration.

reaction to determine if the consumption is complete.<sup>22</sup> It is difficult to use this band in situ to examine the consumption of  $\text{AuCl}_4^-$  during the reaction because the PANI can have bands that overlap with those of the reactants. For example, PANI (emeraldine salt) has a  $\pi-\pi^*$  transition between 320 and 360 nm and a polaron- $\pi$  transition band at approximately 440 nm that can shift depending on the solution conditions.<sup>29-31</sup> In fact, spectral shifts for the polaron transition are common and indicate oxidative or morphological changes in the polymer.<sup>32-35</sup>

The time-dependent changes of the reaction mixture containing aniline and  $\text{AuCl}_4^-$  in 0.10 M  $\text{HBF}_4$  solution are presented in parts c ( $t = 10$  s) and d ( $t = 70$  s), respectively, of Figure 1. Two bands associated with the product are observed at 381.3 and 727.5 nm. The assignment of the band located at 381.3 nm is difficult because it lies between the  $\pi-\pi^*$  transition of the benzene ring for the polymer and the band associated with the polaron- $\pi$  transition. The band at 727.5 nm has been assigned previously to the localized polaron- $\pi^*$  transition of the polymer.<sup>31-34</sup> This band is also known to shift in wavelength as a function of structural and oxidative changes.<sup>28-30</sup> The bands at 381.3 and

(29) Higuchi, M.; Imoda, Daisuke, Hiroa, T. *Macromolecules* **1996**, *29*, 8277.

(30) Venugopal, G.; Quan, X.; Johnson, G. E.; Houlihan, F. M.; Chin, E.; Nalamasu, O. *Chem. Mater.* **1995**, *7*, 271.

(31) Neoh, K. G.; Young, T. T.; Looi, N. T.; Kang, E. T.; Tan, K. L. *Chem. Mater.* **1997**, *9*, 2906.

(32) Han, C.-C.; Hong, S.-P. *Macromolecules* **2001**, *34*, 4937.

(33) Wang, P.; Tan, K. L.; Zhang, F.; Kang, E. T.; Neoh, K. G. *Chem. Mater.* **2001**, *13*, 581.

(34) Albuquerque, J. E.; Mattoso, L. H. C.; Balogh, D. T.; Faria, R. M.; Masters, J. G.; MacDiarmid, A. G. *Synth. Met.* **2000**, *113*, 19.

(35) Wei, Y.; Hsueh, K. F.; Jang, G.-W. *Macromolecules* **1994**, *27*, 518.



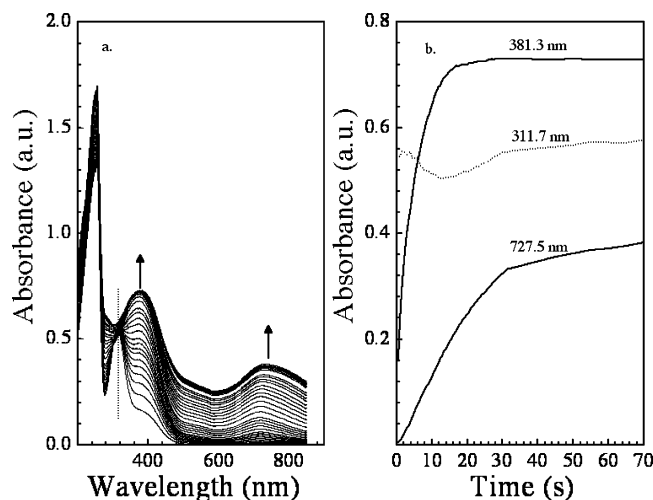


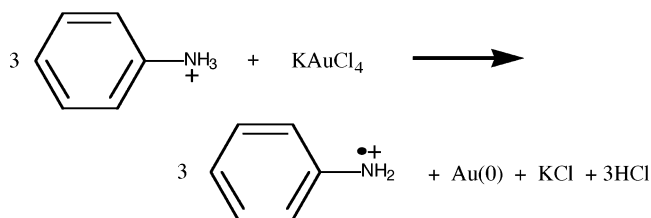
**Figure 2.** (a) In situ UV/vis spectra of a mixture of 0.20 mL of  $2.50 \times 10^{-2}$  M  $\text{KAuCl}_4$  and 3 mL of 0.02 M aniline both in 0.1 M  $\text{HBF}_4$ . The data shown include spectra obtained from 0.5 to 5.0 s (0.5 s intervals), from 6 to 10 s (1 s intervals), from 12 to 32 s (2 s intervals), and from 45 to 70 s (15 s intervals). Arrows indicate the direction of band growth as a function of time. The dashed line passes through the center of the  $\text{AuCl}_4^-$  band at 311.7 nm. (b) UV/vis absorbance intensity versus time for the absorbance bands for  $\text{AuCl}_4^-$  (311.7 nm) and product bands (381.3 and 727.5 nm).

727.5 nm were used to monitor the formation of PANI (in situ) during the polymerization process.

The degree of  $\text{AuCl}_4^-$  reduction and formation of polymer and residual oligomeric material in the system was determined using the filtrate from the reaction shown in Figure 1e. The benefit of examining the filtrate is that the overlapping bands associated with the polymer are eliminated, leaving any unreacted aniline and  $\text{AuCl}_4^-$  behind. Excess aniline is clearly observed in the filtrate spectrum. In addition a small shoulder exists possibly due to residual  $\text{AuCl}_4^-$  in solution. However, the amount of gold species remaining is considered to be negligible to provide an estimate of the theoretical weight percent of gold in the PANI. With this assumption we find the weight percent of the gold is on the order of 60% in PANI. This value will be compared to an estimate of the percent gold from elemental analysis and XPS data.

**In Situ UV/Vis Spectroscopy of PANI/Au Composite Synthesis.** The in situ studies were performed using a mixture of 0.20 mL of  $2.50 \times 10^{-2}$  M  $\text{KAuCl}_4$  and 3.00 mL of 0.02 M aniline in 0.10 M  $\text{HBF}_4$ . A large excess of aniline was used in comparison to  $\text{AuCl}_4^-$  to facilitate the complete reduction of  $\text{AuCl}_4^-$  in the solution. The mixed absorption bands of both aniline and  $\text{AuCl}_4^-$  are observed between 200 and 290 nm in Figure 2a. We expect the absorbance bands for both species to decrease as the aniline monomer and gold species are consumed during the reaction. However, we find that the band for aniline actually increases over the first 70 s. Over the same period of time the characteristic  $\pi-\pi^*$  and polaron- $\pi$  bands associated with the polymer emerge as PANI is formed in the solution. On the basis of these initial results, it is not apparent that the consumption of  $\text{AuCl}_4^-$  and aniline and the formation of the polymer in solution are linked. However, the isolated absorbance for  $\text{AuCl}_4^-$  ( $\lambda = 311.7$  nm) over the first 20 s displays an initial drop consistent

with the consumption of this species from solution (Figure 2b). The increase in intensity of the aniline band can be attributed to the formation of colloidal gold in solution based on the following reaction:



The gold particles remain suspended in solution, causing an increase in the amount of light scattering. This increase causes a shift in the baseline of each spectrum to higher intensity. This trend is observed in Figure 2a, which shows that the spectra shift to higher absorbance as the concentration of the colloidal gold increases during the reaction. The trend is also repeated for the aniline/ $\text{AuCl}_4^-$  combination absorbance bands and the bands associated with the formation of PANI. Quantitative analysis of the species concentrations is not possible at this point in the reaction due to the large degree of light scattering by the colloidal gold in solution. However, reaction trends for the products can be monitored during the reaction at  $\lambda = 381.3$  and 727.5 nm, in Figure 2b.

Assignment of the species giving rise to the band at 381.3 nm is based on previous UV/vis analysis of solutions containing only the aniline trimer or tetramer, which have broad absorbance bands between 360 and 400 nm.<sup>36</sup> In addition, Wei and co-workers also monitored the initial reaction products from the electrochemical formation of short-chain polymer structures and PANI using UV/vis. Their results suggest that the formation of long polymer chains occurs after short-chain intermediate structures are formed in the solution.<sup>37</sup> In fact, the reaction of aniline to form short-chain-length structures such as dimers, trimers, and tetramers was considered by Wei and co-workers to be the rate-limiting step in the formation of PANI.<sup>37</sup> Spectroelectrochemical analysis of PANI by Genies and co-workers also suggests that UV/vis bands below 400 nm are primarily due to soluble polymer intermediates with a small contribution from larger polymer units.<sup>38</sup>

The UV/vis data for the two species indicate that the band for short-chain oligomers located at 381.3 nm emerges  $\sim 2$  s before the absorbance for the long-chain polymer species observed at 727.5 nm. There is also a difference in the initial rate of formation of short-chain species,  $9.5 \times 10^{-2} \text{ s}^{-1}$  (381.3 nm), and the long-chain polymer,  $4.0 \times 10^{-3} \text{ s}^{-1}$  (727.5 nm), at 2.5 s. Although the values represent simple rates of formation based on the change in absorbance versus time for each species, the difference suggests that the reduction of  $\text{AuCl}_4^-$  and formation of oligomeric species is initially the dominant process in the reaction.

(36) Boyer, M. I.; Quillard, S.; Cochet, M.; Louarn, G.; Lefrant, S. *Electrochim. Acta* **1999**, *44*, 1981.

(37) Wei, Y.; Tang, X.; Sun, Y. *J. Polym. Sci., Part A: Polym. Chem.* **1999**, *27*, 2385.

(38) Genies, E. M.; Boyle, A.; Lapkowski, M.; Tsintavis, C. *Synth. Met.* **1990**, *36*, 139.

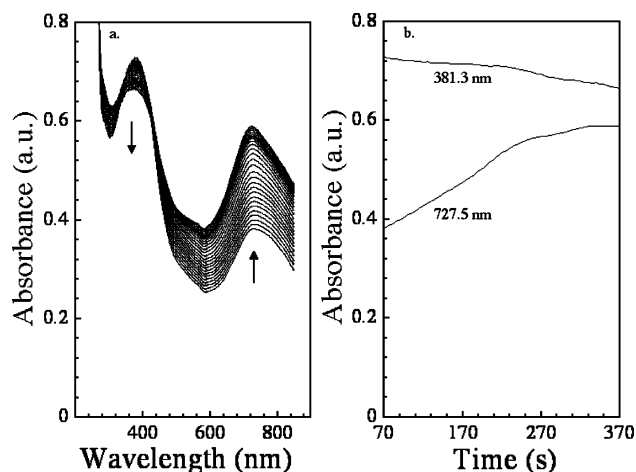


**Figure 3.** (a) Continued reaction of the mixture from Figure 2 at times 70–370 s (10 s intervals). Arrows indicate the direction of band growth as a function of time. (b) Time-dependent UV/vis absorbance intensity for the product absorbance bands (381.3 and 727.5 nm).

Significant changes in the absorbance bands are observed in Figure 3 after the first 70 s. The absorbance for short-chain intermediates (381.3 nm) decreases, while the band at 727.5 nm continues to increase in intensity. We find that the rate of formation of short-chain intermediate structures observed at  $\lambda = 381.3$  reaches zero at  $\sim 20$  s. After  $\sim 20$  s the rate of formation for the short-chain intermediates is negative, indicating that the species concentration is decreasing in solution. For example, the rate is  $-2.8 \times 10^{-6} \text{ s}^{-1}$  at 70 s, reaching a value of  $-2.3 \times 10^{-4} \text{ s}^{-1}$  at 370 s. In contrast, the rate of formation for long-chain polymer species is positive ( $6.9 \times 10^{-5} \text{ s}^{-1}$ ) at 70 s and 0 M/s at 370 s. This trend is consistent with the formation of the long-chain polymeric units with growth facilitated by the consumption of short-chain intermediate structures from the solution.<sup>37,38</sup>

Termination of the synthetic process can be attributed to two related processes. First, the continued reduction of  $\text{AuCl}_4^-$  and formation of intermediates ceases when the gold species is consumed. In addition, the reaction of these intermediate units to form long PANI chains slows and ceases as the intermediates are consumed. It is not clear from the spectroscopic data when  $\text{AuCl}_4^-$  is completely consumed due to the overlap between the absorbance bands of the intermediates. However, once the reduction of the  $\text{AuCl}_4^-$  ceases, the reaction of intermediate structures to form long-chain structures becomes dominant. Precipitation of the PANI composite from solution occurs when the solubility limit is exceeded. In the case of the chemical synthesis the precipitation of PANI is solely related to the lack of solubility of PANI in aqueous solvent as the chain length of the polymer becomes large.

In our system the interaction of the polymer with the gold particles in solution is also an issue. The nucleation of PANI onto platinum and gold electrodes is well-known and an integral part of the formation of PANI membranes at electrochemical interfaces.<sup>39–41</sup> Nucleation of the forming polymer in solution onto the

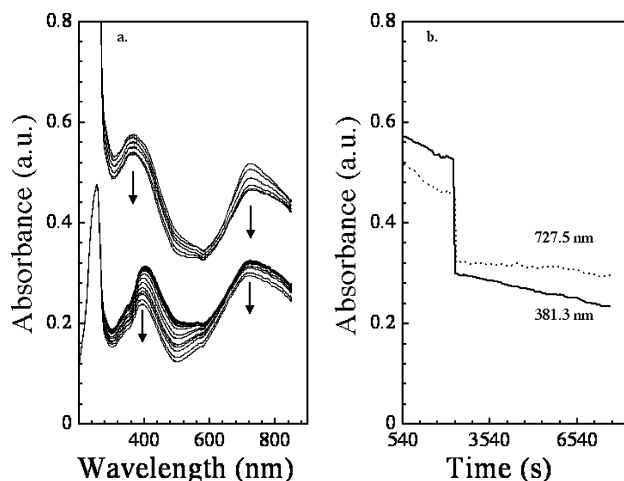


**Figure 4.** (a) Continued reaction of the mixture from Figure 2 at times 540–2340 s (300 s intervals), 2340–2940 s (60 s intervals), and 3240–7380 s (600 s intervals). Arrows indicate the direction of band growth as a function of time. (b) Time-dependent UV/vis absorbance intensity for the product absorbance bands (381.3 and 727.5 nm).

colloidal gold likely contributes to the material's lack of solubility. The UV/vis spectra displayed in Figure 4a show the precipitation of PANI from solution. In this figure, selected spectra are shown for the reaction, which was monitored every 60 s from 420 to 7680 s. The data show a decrease in both species bands at 381.3 and 727.5 nm (Figure 4b). A rapid decrease in the intensity of the signal is observed between 2280 and 2340 s due to the composite precipitation, which is marked by the appearance of a diminished aniline and background signal.

The diminished background signal is primarily the result of a decrease in light scattering associated with the loss of gold colloids in solution. This behavior suggests that the polymer and gold are not independent species in the solution and precipitate together. It is interesting to note that not all of the polymeric material has precipitated at the end of this experiment (time 7680 s). However, if the solution is allowed to sit for a few additional hours, the signal approaches the baseline, leaving the signature of unreacted aniline in the solution (Figure 1e).<sup>22</sup> The UV–vis spectrum taken of the solution does not show any appreciable amount of  $\text{AuCl}_4^-$ , indicating that the gold species is consumed in the reaction.

**Mechanism for the Formation of PANI/Au Composites.** The interaction of conducting polymers with  $\text{AuCl}_4^-$  has been examined previously by a number of groups. In each case the polymer was produced separately and then reacted with  $\text{AuCl}_4^-$ .<sup>18,20–22</sup> In a recent study of the chemical synthesis of a polypyrrole/Au composite the formation of colloidal polypyrrole was accomplished using ferric chloride as the oxidant prior to the introduction and reduction of the  $\text{AuCl}_4^-$ .<sup>42</sup> Our system is unique because the PANI/Au composite is formed without the aid of any chemical species other than the  $\text{AuCl}_4^-$  anion and aniline.

(39) Diaz, A. F.; Logan, J. A. *J. Electroanal. Chem.* **1980**, *111*, 111.

(40) Genies, E. M.; Tsintavis, C. *J. Electroanal. Chem.* **1985**, *195*, 109.

(41) Genies, E. M.; Syed, A. A.; Tsintavis, C. *Mol. Cryst. Liq. Cryst.* **1985**, *121*, 181.

(42) Henry, M. C.; Hsueh, C.-C.; Timko, B. P.; Freund, M. S. *J. Electrochem. Soc.* **2001**, *148*, D155.

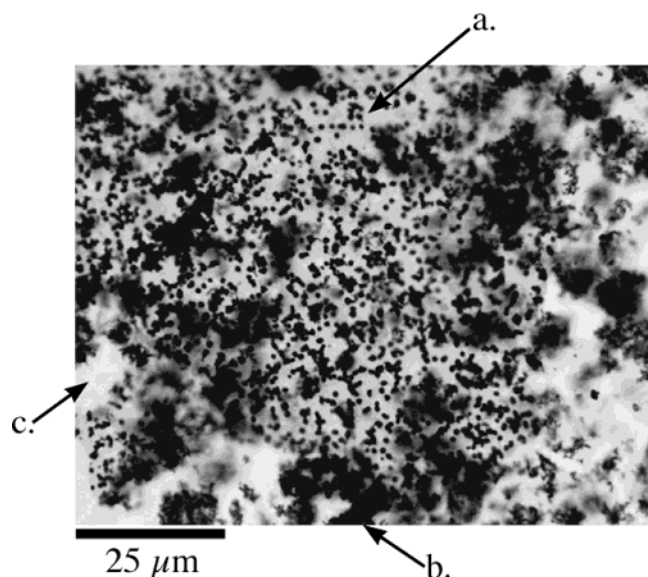


**Figure 5.** Optical image (100 $\times$ , reproduced at 74% of original size) of the Au/PANI composite in the reaction solution using transmitted light: (a) gold particles (black dots) encapsulated by polymer (light gray); (b) optically dense region of the PANI/Au composite; (c) void space (absence of Au(0) or PANI).

The chemical synthesis of the PANI using  $\text{AuCl}_4^-$  is similar to the chemical synthesis of PANI using a more common oxidizing agent such as peroxydisulfate. Our spectroscopic data indicate that  $\text{AuCl}_4^-$  produces intermediate species in solution that are used as building blocks in the polymerization reaction. Our spectroscopic data suggest that consumption of the intermediate species is critical in the formation of PANI. Although we believe that the mechanism of PANI formation is very similar to that described by Wei, Genies, and co-workers, there is one significant difference.<sup>37,38</sup> In the previous studies polymer nucleation and growth occurred at a poised electroactive surface which facilitated the controlled, sequential growth of a polymer membrane. In our studies the in situ nucleation and growth of the polymer onto colloidal metallic surfaces represents a significant deviation from the previous studies of the chemical and electrochemical formation of PANI and PANI/metal composites.

**PANI/Au Characterization. Imaging and Diffraction of PANI/Au Composites.** Precipitation of the PANI/Au composite suggests that there is significant interaction between the gold particle and the polymer in solution. However, questions regarding the final oxidation state of the metal species, the distribution, and the physical and chemical relationship between the gold and the polymer remain unanswered. Therefore, optical images were obtained of the PANI/Au composite in situ to examine the dispersion and incorporation of metal species in the polymer while still in solution.

Examination of the reaction product using an optical microscope in the transmission mode reveals that the PANI/Au composite in the solution encapsulates the gold particles. Gold particles appear as uniformly dispersed dark spots in the polymer matrix with an average diameter of  $\sim 1 \mu\text{m}$  (Figure 5a). It is impossible to sample and resolve the entire three-dimensional structure using optical objectives in transmitted mode, and some optically dense regions are clearly observed

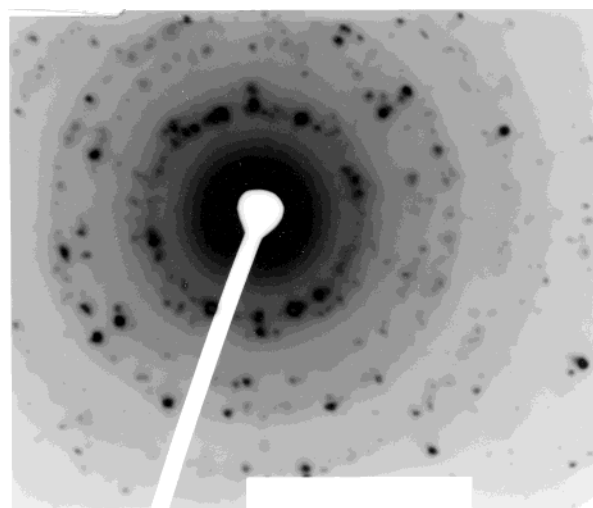


**Figure 6.** Transmission TEM diffraction image obtained from the PANI/Au composite.

in the image (Figure 5b). In addition, the image shows regions where no PANI/Au is present (Figure 5c). The uniformity of the polymer coating on the metal is difficult to gauge from the optical images. However, optical studies of the filtered, dry material have shown a small amount of exposed metallic species exist at the polymer surface (image not shown). The data suggest that the polymer coating on the metal is not uniform and that some free Au surface area does exist.

The crystal structure of the gold particles encapsulated by PANI was also examined using TEM diffraction. The use of TEM diffraction in Figure 6 provides information regarding both the polymer and the metallic particles. From the diffraction pattern two clear conclusions can be drawn. First, the polymer is amorphous, producing the characteristic rings in the diffraction pattern. More importantly, the gold particles in the PANI are not amorphous. The metallic diffraction pattern is in the form of spots superimposed on the rings. This is consistent with diffraction by many different crystallographic orientations. From the data it is clear that the composite consists of amorphous PANI with encapsulated polycrystalline gold particles.

**FTIR Spectroscopy of PANI/Au Composites.** FTIR analysis of the fingerprint region between 700 and 1600  $\text{cm}^{-1}$  is particularly useful for examining the resonance modes of the benzenoid and quinoid units, and individual bonds (i.e., out-of-plane C–H and C–N) of PANI.<sup>21,39,43</sup> The FTIR spectra of pure PANI/HBF<sub>4</sub> and PANI/Au are presented in Figure 7. The characteristic ring bands for aromatic C–C stretching are located at 1597 and 1512  $\text{cm}^{-1}$  versus 1593 and 1510  $\text{cm}^{-1}$  for the pure polymer and the composite, respectively. In addition, the IR bands for the out-of-plane C–H are in good agreement with values of 832 and 829  $\text{cm}^{-1}$  for PANI/HBF<sub>4</sub> and PANI/Au. The shifts are well within the 4  $\text{cm}^{-1}$  resolution used for data acquisition.

The characteristic bands associated with the benzenoid phenyl ring ( $\sim 1500 \text{ cm}^{-1}$ ) and quinoid phenyl ring ( $\sim 1590 \text{ cm}^{-1}$ ) of the polymer are labeled in the figure. These bands can be used to estimate the oxidation state of the polymer, where the percent oxidized

(43) Hatchett, D. W.; Josowicz, M.; Janata, J. *J. Phys. Chem. B* 1999, 103, 10992.



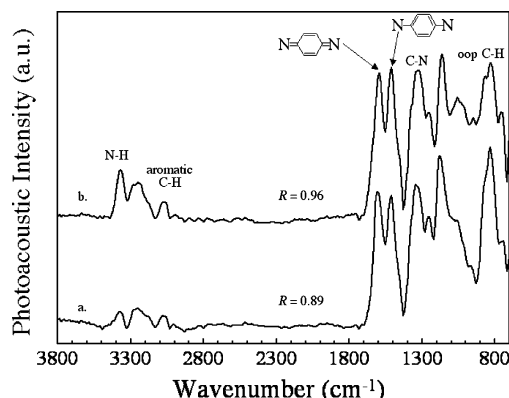
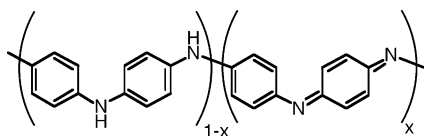


**Figure 7.** Photoacoustic FTIR spectra of (a) pure PANI/HBF<sub>4</sub> (without Au particles) and (b) the PANI/Au composite produced during chemical synthesis using AuCl<sub>4</sub><sup>−</sup> as the oxidant. FTIR band assignments and the ratio *R* of the reduced and oxidized units are labeled for clarity.

units, *x*, versus reduced units, 1 − *x*, is obtained by integrating the IR bands as shown in the following schematic:<sup>23,41</sup>



where

$$R = \frac{1 - x}{x} = \frac{\text{area}_{\text{reduced}}}{\text{area}_{\text{oxidized}}} = \frac{\text{area}_{\nu(1590\text{cm}^{-1})}}{\text{area}_{\nu(1500\text{cm}^{-1})}}$$

For emeraldine salt the integrated peaks have shown that the benzenoid and quinoid units are approximately equal (i.e., *R* ≈ 1). Integration of the peaks for PANI/HBF<sub>4</sub> and PANI/Au gives values of *R* = 0.96 and 0.89, respectively. These values correspond to 49/51 and 47/53 ratios of benzenoid/quinoid units in the polymer. The data suggest that each material contains nearly identical percentages of oxidized and reduced units.

The effect of Au on the oxidized and reduced units within the polymer is fairly small. However, a significant shift for the semiquinoid C–N stretch is observed when the two materials are compared. The band is located at 1335 cm<sup>−1</sup> for PANI/HBF<sub>4</sub>, shifting to lower energy (1323 cm<sup>−1</sup>) for PANI/Au. The 12 cm<sup>−1</sup> shift to lower energy is significant because it is directly related to differences in chemistry and electron density at the nitrogen group. The data indicate that the C–N bonds (or amino and imino bonds) within the polymer are influenced by the gold particles. The energy shift indicates that the Au directly influences the electron density of the C–N bond. The shift to lower energy suggests that Au donates electron density to the imino nitrogen in the polymer. The interaction of the Au with nitrogen groups is also consistent with the nucleation of PANI onto gold. It is interesting to note that no large change in the energy for the N–H band is observed (3373 and 3369 cm<sup>−1</sup>). It is likely that the electron density of the C–N bond is more strongly perturbed by the presence of the gold particles in the PANI matrix.

**Elemental Analysis.** Polyaniline is synthesized in emeraldine salt form, with protonation occurring mainly

**Table 1.** PANI/HBF<sub>4</sub> and PANI/Au Elemental Analysis (C, H, N, F, S, Cl, B, O) normalized to N = 1.0<sup>a</sup>

element	% composition	no. of moles	mole ratio	analysis ratio
(a) PANI/HBF <sub>4</sub>				
C	61.14	5.09	6.10	C <sub>6.10</sub> H <sub>4.98</sub> N <sub>1.00</sub> F <sub>0.41</sub> S <sub>0.22</sub> B <sub>0.11</sub> O <sub>0.72</sub>
H	4.68	4.16	4.98	
N	13.03	0.83	1.00	
F	7.28	0.34	0.41	
S	6.39	0.18	0.22	
Cl	0.00	0.00	0.00	
B	0.97	0.09	0.11	
O	10.01	0.63	0.72	
(b) PANI/Au				
C	64.68	5.82	6.19	C <sub>6.19</sub> H <sub>4.74</sub> N <sub>1.00</sub> F <sub>0.62</sub> Cl <sub>0.11</sub> B <sub>0.16</sub> O <sub>0.29</sub>
H	4.16	4.46	4.74	Au composition
N	12.19	0.94	1.00	54 wt %
F	10.20	0.58	0.62	
S	0.00	0.00	0.00	
Cl	3.28	0.09	0.11	
B	1.50	0.14	0.16	
O	4.00	0.25	0.29	

<sup>a</sup> The oxygen content is estimated using the O/N ratio from XPS data.

at the imine sites and the counterions supplied by the protonic acid<sup>44</sup> or chemical oxidant.<sup>45</sup> The elemental analysis of pure PANI/HBF<sub>4</sub> and PANI/Au (with HBF<sub>4</sub>) was conducted to determine the chemical composition of the organic component in each sample and to estimate the percent gold in the sample. It can be assumed that the stoichiometric amount of the gold delivered was consumed in the reaction since the solution did not contain any AuCl<sub>4</sub><sup>−</sup> after the filtration (Figure 1e). The elements C, N, H, Cl, F, B, O, and S accounted for 46% of the total mass for the PANI/Au composite. The oxygen content was estimated from the XPS data using the integrated ratio of nitrogen and oxygen, where O/N = 0.29. The remaining mass was attributed to the mass of Au in the sample at 54%. This value is consistent with the theoretical value of 60% based on the number of moles of the limiting reagent AuCl<sub>4</sub><sup>−</sup> used in the chemical synthesis.

The unit formula consistent with the emeraldine form of polyaniline, C<sub>6</sub>H<sub>4.5</sub>N, is based on an equal number of oxidized and reduced units in the polymer, excluding proton doping.<sup>49</sup> The hydrogen value of greater than 4.5 from the elemental analysis can be attributed to the degree of proton doping. In addition, any excess proton in the system requires the uptake of anions to maintain charge neutrality. Anion uptake can be in the form of the common ion Cl<sup>−</sup> from AuCl<sub>4</sub><sup>−</sup> reduction or BF<sub>4</sub><sup>−</sup>. In the case of the PANI/HBF<sub>4</sub> composite products from the reduction of peroxydisulfate can also contribute to the anion doping.<sup>45</sup> The balancing of the charge associated with the proton doping is achieved through the uptake of anions in the system. Therefore, the relative charge of the excess proton and anion present will be compared using the data from the elemental analysis of PANI/HBF<sub>4</sub> and PANI/Au in Table 1.

Elemental analysis of PANI/HBF<sub>4</sub> in Table 1a provides a unit formula for PANI synthesis using peroxydisulfate (C<sub>6.10</sub>H<sub>4.98</sub>N<sub>1.00</sub>B<sub>0.11</sub>F<sub>0.41</sub>S<sub>0.22</sub>O<sub>0.72</sub>). A value of ~5.0 for hydrogen indicates that the polymer is proton

(44) MacDiarmid, A. G.; Xiang, J. C.; Richter, A. F.; Epstein, A. J. *Synth. Met.* **1987**, *18*, 285.

(45) Inoue, M.; Navarro, E. R.; Inoue, M. B. *Synth. Met.* **1989**, *30*, 199.



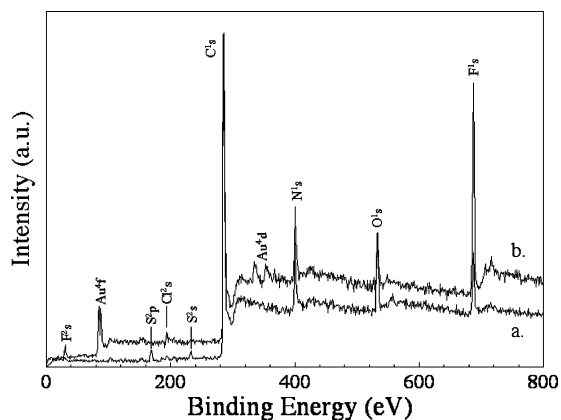


**Figure 8.** XPS surveys of the (a) PANI/HBF<sub>4</sub> and (b) PANI/Au composites. The XPS peaks are labeled for clarity.

doped (0.5). The data also show that the polymer contains anions consistent with both the protic acid HBF<sub>4</sub> and the chemical oxidant S<sub>2</sub>O<sub>8</sub><sup>2-</sup>. The value obtained for F (0.41) must be divided by 4 to take into account the stoichiometry of the BF<sub>4</sub><sup>-</sup> anion as an estimate of the charge (0.1). A significant amount of S was also found in the polymer (0.22), indicating that the reduced peroxydisulfate plays a role in the doping. For comparison, the concentration of HBF<sub>4</sub> is 1 M, while the concentration of peroxydisulfate is 0.25 M. However, the reduction of one peroxydisulfate ion during the aniline oxidation results in the formation of two SO<sub>4</sub><sup>2-</sup> anions in the solution (~0.5 M), which can readily act as a dopant in the polymer.<sup>45</sup> On the basis of the 2-fold difference in concentration between the anions present in solution, the polymer shows moderately higher affinity for SO<sub>4</sub><sup>2-</sup> in comparison to BF<sub>4</sub><sup>-</sup>. The contribution from SO<sub>4</sub><sup>2-</sup> in terms of the charge would be on the order of 0.44. The overall anion doping charge (0.10, BF<sub>4</sub><sup>-</sup>; 0.44, SO<sub>4</sub><sup>2-</sup>) of 0.54 is consistent with the degree of proton doping (0.5) for the system.

Elemental analysis of PANI/Au in Table 1b provides a unit formula for PANI synthesis using AuCl<sub>4</sub><sup>-</sup> (C<sub>6.19</sub>H<sub>4.74</sub>N<sub>1.00</sub>B<sub>0.16</sub>F<sub>0.62</sub>Cl<sub>0.11</sub>O<sub>0.29</sub>, with no S detected). The degree of proton doping for the PANI/Au composite is smaller than that for PANI/HBF<sub>4</sub>. A value of 0.24 is obtained for the degree of proton doping in the PANI/Au system. In the case of PANI/Au there are two possible anion dopants present in the form of BF<sub>4</sub><sup>-</sup> and Cl<sup>-</sup>. The presence of chloride in the PANI/Au system is a direct result of the reduction of AuCl<sub>4</sub><sup>-</sup> to Au(0) (four Cl<sup>-</sup> anions released into solution) during the oxidative polymerization of aniline (see the reaction scheme). It is also possible that a small amount of Cl<sup>-</sup> is physisorbed to the crystalline Au in the system. The exact distribution of Cl<sup>-</sup> between these phases is unknown. However, if we assume Cl<sup>-</sup> acts primarily as a polymer dopant, the contribution for BF<sub>4</sub><sup>-</sup> and Cl<sup>-</sup> is 0.16 and 0.11, providing an overall contribution of 0.27 for the anion dopant charge. This value is consistent with the proton doping calculated for the system (0.24). In addition, the data indicate that in PANI/Au the overall proton/anion doping is reduced in comparison to that in PANI/HBF<sub>4</sub>.

**X-ray Photoelectron Spectroscopy.** The photoelectron spectra of PANI/HBF<sub>4</sub> and PANI/Au are shown in parts a and b, respectively, of Figure 8. XPS provides infor-

mation concerning the density of occupied electronic states at the surface of the sample. The XPS spectra support the data obtained from TEM diffraction, Figure 6, which demonstrates the crystalline nature of Au embedded in PANI, where the electron diffraction pattern is indicative of the presence of gold species in PANI. The presence of metallic gold in the PANI/Au XPS spectrum is marked by the appearance of a sharp doublet emission peak for Au(0) located at 84.4 eV (<sup>4</sup>f<sub>7/2</sub>) and 88.1 eV (<sup>4</sup>f<sub>5/2</sub>). The binding energy values are consistent with the previously determined energies for metallic gold in PANI.<sup>21</sup> Any AuCl<sub>4</sub><sup>-</sup> present in the polymer would give rise to XPS peaks for Au(III) in the form of a doublet at 87 eV (<sup>4</sup>f<sub>7/2</sub>) and 92 eV (<sup>4</sup>f<sub>5/2</sub>).<sup>22</sup> The absence of any peak at 92 eV indicates that no Au(III) species exist in the polymer. The high ratio, N/Au = 8, calculated from the XPS data, given the sensitivity factors for N (0.42) and Au (2.8),<sup>46</sup> indicates that most of the gold occurs in the bulk of the PANI sample rather than at the polymer surface for the PANI/Au composite. The data support the encapsulation of gold particles by the forming polymer prior to precipitation.

The N 1s count rates in both of the samples are of approximately equal magnitude, indicating that the amounts of sample exposed to the beam in each sample are roughly equivalent. The survey of PANI/HBF<sub>4</sub> shows fluorine and sulfur associated with the acid and ammonium peroxydisulfate used in the polymerization reaction. In contrast, the scan for PANI/Au shows only the resolved fluorine signature of HBF<sub>4</sub>. The chloride ion is observed as a poorly resolved band above the baseline at ~195 eV (Cl 2s) and provides only qualitative information concerning the presence of Cl<sup>-</sup> in PANI/Au (Figure 8b). The low signal-to-noise ratio for Cl is expected on the basis of the low Cl/N ratio calculated from elemental analysis (0.11) and low XPS sensitivity of the ion (0.37).<sup>46</sup>

The identification of F is straightforward with a strong emission peak at 687 eV for both materials. From the elemental analysis data we found that the PANI/HBF<sub>4</sub> composite had a smaller percentage of F in comparison to PANI/Au. The ratio of F to N for both samples was calculated from the XPS spectral areas after correction with sensitivity factors (F, 1; N, 0.42),<sup>46</sup> and the stoichiometry of the doping species (four F atoms per BF<sub>4</sub><sup>-</sup> anion). Single Gaussian integration of the spectral area of nitrogen and fluorine from the XPS data provides an estimate of the degree of doping by BF<sub>4</sub><sup>-</sup> with values of 0.10 and 0.24 for PANI/HBF<sub>4</sub> and PANI/Au, respectively. The value of 0.10 for PANI/HBF<sub>4</sub> agrees favorably with the value from elemental analysis (0.10). A higher doping of BF<sub>4</sub><sup>-</sup> for PANI/Au is obtained from XPS as compared to the value of 0.16 obtained from elemental analysis data and likely represents a higher concentration of the species at the surface.

In the case of PANI/HBF<sub>4</sub>, the low-energy sulfur peaks centered at 164 eV (S 2p) and 230 eV (S 2s) can also be identified in Figure 8a. The atomic ratio O/S = 3.4, calculated from the XPS data in Figure 8a using the S 2s sensitivity of 0.33, is in good agreement with the ratio O/S = 4 for the SO<sub>4</sub><sup>2-</sup> anion. Furthermore, a comparison of S/F from elemental and XPS analysis

(46) Wagner, C. D.; Davis, L. E.; Zeller, M. V.; Taylor, J. A.; Raymond, R. M.; Gale, L. H. *Surf. Interface Anal.* **1981**, *3*, 211.

provides a measure of the relative doping between the two possible anions with comparable values of 0.5 (elemental) and 0.6 (XPS) for PANI/HBF<sub>4</sub>. The results indicate that both HBF<sub>4</sub> and SO<sub>4</sub><sup>2-</sup> play roles as counterions in the doping of PANI/HBF<sub>4</sub>.

**Electronic Resistance/Conductance.** The synthesis of PANI/Au was carried out in the presence of 1 M HBF<sub>4</sub> to ensure the polymer would be proton doped. It has been reported that the conductivity of PANI increases 6-fold as a function of pH decreasing from 6 to 0.<sup>47</sup> The range of conductance values for PANI doped with HCl has been reported to be between 2 and 10 S/cm in the literature for multiple synthetic processes.<sup>48</sup> Optimization of the synthetic conditions has shown that the highest conductivity is obtained when the polymer contains a dopant/N ratio of 0.5 and an equal number of oxidized and reduced units.<sup>49</sup> The conductance value for PANI/HBF<sub>4</sub><sup>-</sup> (9.0 S/cm  $\pm$  10%) is in agreement with this observation. Our results also indicate that the combined doping ratio is on the order of 0.3 for PANI/Au. In addition, the FTIR analysis of the material indicates that the polymer consisted of an equal number of oxidized and reduced units. The four-point probe sheet conductance for a pressed pellet of PANI/Au using the four-point probe is 3.2 S/cm  $\pm$  12%. For comparison, the conductance measured for PANI/Au without HBF<sub>4</sub> was  $4.4 \times 10^{-7}$  S/cm. The results indicate that insertion of Au metal in the polymer and the small decrease in proton/anion doping associated with the process do not

result in a large decrease in the conductivity for the material. However, proton doping is still critical in maintaining the conductance of PANI/Au. The data suggest that the single-step synthesis of highly conductive PANI/metal composites is possible using AuCl<sub>4</sub><sup>-</sup> as the monomer oxidant in the presence of acid.

## Conclusions

This study has shown that AuCl<sub>4</sub><sup>-</sup> is a suitable oxidizing agent for the direct chemical polymerization of aniline. The formation of the PANI/Au composite proceeds until all of the AuCl<sub>4</sub><sup>-</sup> and radical aniline species in solution are consumed. Precipitation of the composite occurs as the polymer chain length increases and the solubility limit of the polymer/metal composite is exceeded. Optical images clearly show polymer-encapsulated gold particles that are uniformly distributed throughout the material. In addition, optical and TEM images indicate the particle diameter is relatively constant ( $\sim 1 \mu\text{m}$ ). This synthesis provides a new method for producing gram quantities of polymer/metal composite materials with high metal content (up to  $\sim 54$  wt %) and chemical reproducibility. Moreover, the results suggest that the gold does not adversely affect the electronic properties of the polymer. The composite conductance is comparable to that of the chemically produced PANI/HBF<sub>4</sub> despite the decreased proton and anion doping.

**Acknowledgment.** We acknowledge Dr. Dennis Lindle and Dr. Allen Johnson for their help in obtaining the XPS results. The research was supported by NSF EPSCoR/Nevada. This work was also supported by the National Science Foundation, Grant No. CHE-9816017.

CM049478I

(47) Travers, J. P.; Chroboczek, F.; Devereux, F.; Genoud, F.; Nechtschein, M.; Syed, A. A.; Genies, E. M.; Tsintavis, C. *Mol. Cryst. Liq. Cryst.* **1985**, *121*, 195.

(48) Stejskal, J.; Gilbert, R. G. *Pure Appl. Chem.* **2002**, *74*, 857.

(49) Ray, A.; Richter, A. F.; MacDiarmid, A. G.; Epstein, A. J. *Synth. Met.* **1989**, *29*, E151.